

Seeking Globular Clusters: M2 and Future Observations

Rubait U. Ahamed,¹*

¹*Department of Physics, Faculty of Science, University of Manitoba, CA*

Accepted XXX. Received 16th DEC 2024; in original form 12 DEC 2024

ABSTRACT

We present detailed observations of the Messier 2 globular cluster in two photometric bands. Our study involves developing a customized data reduction pipeline in Python to process raw images effectively and derive significant results. The primary scientific objective is to construct a Hertzsprung-Russell (H-R) diagram for Messier 2 (M2), which will allow us to estimate the cluster's age. Globular clusters like M2 provide crucial insights into stellar evolution, as they contain some of the oldest stars in the universe. By carefully analysing the photometric data in the B and R Filter, we aim to map the evolutionary stages of these stars accurately. The H-R diagram constructed from our data estimates the age of M2 by extracting the effective temperature and absolute magnitude of the oldest star in the cluster, shedding light on the evolutionary processes at play. Our observations reveal that the oldest star in M2 has a $T_{\text{eff}} \approx 10^3 K$ and $M_B \approx 16.5$. Looking ahead, we plan to apply our developed reduction pipeline and observational techniques to the Messier 13 (M13) globular cluster. This follow-up study aims to verify the robustness of our methods and to expand our understanding of stellar evolution across different globular clusters.

Key words: Astronomy – Globular Clusters – Telescope

1 INTRODUCTION

Globular clusters are densely packed groups of stars, often containing hundreds of thousands of stars within a relatively small volume of space (Gratton et al. (2019)). These ancient stellar systems are of significant scientific interest because they offer a unique window into the early stages of galaxy formation and the evolution of stars. Understanding the properties and behaviours of globular clusters can provide insights into the broader field of astronomy, particularly in the areas of stellar evolution, galactic dynamics, and the chemical enrichment of galaxies.

The target of this study is the globular cluster Messier 2. M2 is particularly notable for its great age and high stellar density, making it an exemplary member of the globular cluster class. (Lardo et al. (2013)) points out that M2 is one of the oldest clusters in our galaxy and is believed to contain multiple populations of stars, which are indicative of complex formation and evolutionary histories. The presence of these multiple stellar populations makes M2 an intriguing subject for study, as it allows for a more detailed examination of the processes that govern the formation and evolution of globular clusters.

Our approach to studying M2, also known as NGC 7089, involves the use of a telescope, equipped with the Johnsons Cousin's B and R filter. We conducted observations in two photometric bands under optimal conditions to ensure high-quality data. A customized data reduction pipeline was developed using Python to process the raw images and extract meaningful results.

This pipeline ensures that our data is accurately reduced, minimiz-

ing errors and enhancing the reliability of our findings. In this paper, we present a detailed analysis of our observations and results. Section 2 outlines the methods used for data acquisition and reduction. Section 3 presents the results of our study, including the construction of a Hertzsprung-Russell diagram for M2, estimation of the cluster's age, and identification of multiple sub-branches within the Red Giant Branch (RGB). Section 4 discusses possible sources of error and future research directions. Finally, Section 5 summarizes our study and its key findings, highlighting the significance of our results within the broader context of globular cluster research.

2 METHODS

In this study, we employed a comprehensive observational and analytical approach to investigate the properties of the M2. Our methodology consisted of carefully planned telescope observations, data acquisition under optimal conditions, and the development of a robust data reduction pipeline. The following sections describe the specific instruments used, the observational conditions, and the procedures followed for data reduction and analysis.

2.1 Observational Techniques

We utilized the Convergent FA12 telescope from AG Optical Systems, featuring a diameter of 317.5mm, a focal length of 1570mm, giving it a f/4.94 ratio, to observe the globular cluster M2. This telescope was equipped with a ZWO ASI6200MM Pro camera, which has 9576 x 6388 pixels, each measuring $3.76\mu m$, and a peak quantum efficiency of 91%.

* E-mail: ahamedru@myumanitoba.ca (RUA)

Our observations were conducted on November 2 and November 5, 2024, under clear skies in New Mexico at a site with a latitude of $32^{\circ} 06' 59''$ N, a longitude of $108^{\circ} 55' 23''$ W, and an elevation of 1290m. The stable atmospheric conditions and elevated site ensured minimal atmospheric interference and giving us a seeing conditions range from about $0.5''$ to $1.5''$. Each observation session had an exposure time of 120 seconds, involving 15 exposures, in both B and R bands, to enhance the signal-to-noise ratio and detect faint stars within the cluster.

Auxiliary equipment included a GM3000 HPS mount from 10Micron, an Optec Gemini focuser with a travel range of 12.7 mm and a drawtube diameter of 95 mm, and an SXCCD Maxi filter wheel loaded with Astrodon L, R, G, B Gen 2, H_{α} , O III, and a dark filters.

Supporting data from [Gaudet et al. \(2020\)](#) further complemented our observations, providing a broader context for our findings and helping to verify the accuracy of our data

2.2 Reduction pipeline

The reduction was carried out in 4 stages. We used VS Code Version 1.95.3 to develop our code in a Jupyter Notebook Python environment. Version 3.12.8 was used for python. All packages referenced in the code used their own respective latest public version

2.2.1 Stacking Obtained Data

Raw images were obtained by our TA from the site location, including 13 dark frames, 65 bias frames, and 15 frames of 120 s exposure time on B and R filters (taken on 2nd and 5th Nov). These images underwent a rigorous data reduction process.

First, the bias and dark frames were stacked to create master bias and master dark frames. Each pixel value was averaged across frames. Then, stacked flat frames were made for each night and filter using the same process. Bias was subtracted from the flats and the results normalized to create 4 master flats (2 nights, 2 filters).

All light frames were corrected by subtracting the master dark and dividing by the corresponding master flat for the filter and day of exposure.

Next, we aligned all B and R filter light frames using the 'align' function from the Astropy package. The first light frame from each night for each filter served as the reference. Following this the light frames stacked, creating 2 master lights for each filter.

The master B and R filter light frames were saved as FITS files. A greyscale plot visualized our progress (as shown in Figure 1).

2.2.2 Analysis of Stacked Data

We loaded the B filter FITS file from our local drive and used the 'find peaks' function from the Twirl package to obtain pixel coordinates of the stars. Only the first 20 hits were kept. We then used the 'gaia radecs' function from Twirl to query the Gaia Archive for RA and DEC of stars around M2. These RA and DEC were used with the 'find peaks' hits to determine the World Coordinate System (WCS) for the detected B filter stars. The FITS file was updated with the new WCS and normalized.

We integrated data from the CANFAR's Stetson database by loading star coordinates and magnitudes, and merging these with the photometric data. Only stars with magnitudes of 18 or brighter were included.

The data was visualized on the B filter image, showing star positions from the Stetson catalogue (Figure A9). We created a cutout

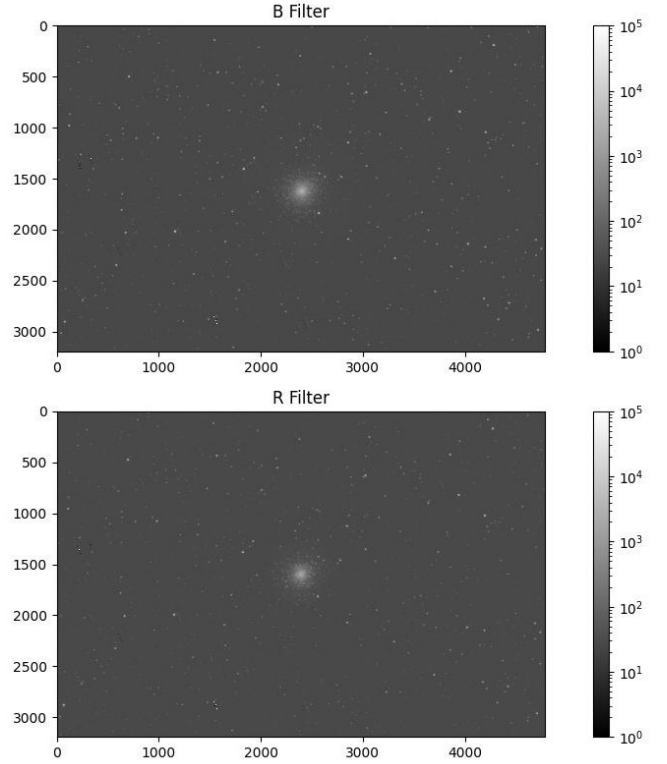


Figure 1. Captured image of M2 on a Logarithmic scale.

of the B filter FITS data for detailed analysis, reran peak detection within this cutout, and recalculated the WCS. The DAOFinder tool detected stars in the cutout, using the DAOFIND algorithm (from [STETSON 1987](#)). The resultant stars are filtered by brightness, and converted into a pandas DataFrame.

Overlaying detected star locations from the Stetson catalogue and DAOFinder tool on the cutout image validated star positions (Figure A1). We updated coordinates from TWIRL with DAOFinder results and matched them with the Stetson catalogue based on celestial coordinates.

A Colour Magnitude Diagram (CMD) was created by calculating the difference between the Stetson R Band and detected B Band magnitudes, providing insights into stellar characteristics (Figure A2). Additionally, a CMD was created using only Stetson catalogue B and R band magnitudes to assess uncertainty (Figure A3).

2.2.3 Creating final Plots

With the magnitude differences from the B and R bands determined, we proceeded to calculate the effective temperature of the detected stars using the Ballesteros formula. [Ballesteros \(2012\)](#) explains that this empirical relation in astronomy converts the B-R colour index of a star to its effective temperature in Kelvin

$$\log(T_{\text{eff}}) = 3.979 - 0.234 \cdot (B - R)$$

where T_{eff} represents the effective temperature and $(B - R)$ denotes the colour index. This formula, grounded in observational data, offers a straightforward method for estimating stellar temperatures based on the B-R colour index.

Given the known distance of M2, approximately 55,000 light years

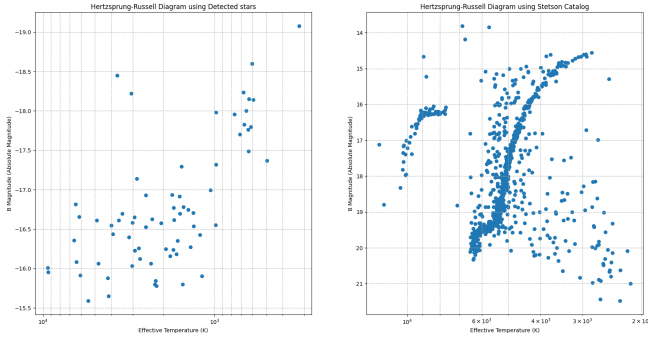


Figure 2. HR Diagram created using detected data VS HR Diagram created using Stetson Catalog data

(Kuzma et al. (2016)), we could calculate the apparent magnitude of each peak. Using the following relation:

$$M = 5 \log_{10}(d) - 5 + m$$

where m is the apparent magnitude, M is the absolute magnitude, and d is the distance to the star in parsecs. Since 1 light year approximately equals 0.3066 parsecs, the distance to M2 in parsecs is 16,863 parsecs.

Armed with the effective temperature and absolute magnitude, we created the Hertzsprung-Russell (HR) diagram displayed in figure A7. This diagram allowed us to visualize and analyse the relationship between the effective temperature and luminosity of the detected stars.

2.2.4 Applying Correction

Upon review, we identified a significant deviation in our detected magnitude data, which was off by 16 magnitudes of the standard deviation of the detected magnitudes. To rectify this, we applied a correction factor to our detected data. This adjustment allowed us to remap the Colour Magnitude Diagram (CMD), as shown in Figure 2 (left) and in Figure A4. This value of 16 was chosen based on the difference in the detected vs the Stetson data that is highlighted in figure A8

By applying this correction, we ensured that our CMD was more accurate and reliable. This process enabled us to proceed with confidence in creating the Hertzsprung-Russell (HR) diagram. The revised HR diagram, which we believe is now corrected for errors, is depicted in Figure 2 (left plot) and figure A6. This adjustment was crucial for maintaining the integrity and accuracy of our analysis, providing a more precise representation of the stellar characteristics in our dataset.

3 RESULTS

We present the HR diagram created using the observed data in the B filter and Stetson's catalogue R filter in figure A6. On the left and HR diagram created using only the Stetsons catalogue data on the right

Using our detected and corrected data, we determined that a star in M2 with a mass similar to the main sequence turnoff mass would have a measured B band magnitude of 16.5 and an effective temperature of 10^3 K.

4 ERRORS AND FUTURE CALIBRATION

As observed from the differences in resolution between the plots in Figures 2, it is apparent that due to poor resolution our estimates may be significantly off. We remark that there is a possibility that our detected data has no stars in the main sequence, but instead are stars on the White Dwarf (WD) branch. Figure 2 illustrates this fact. We also remark that for reasons unknown to us, the absolute detected magnitude has picked up a negative sign. We kept them in our plot, but in the Results and Abstract sections, we decided to quote them without the negative sign as we think these are some kind of errors.

Possible sources of error include Calibration inaccuracies in the photometric data, misalignment of frames during the stacking process or variability in atmospheric conditions during observations. These potential errors were carefully considered in our analysis.

Future research is focused in observing M13 using the same procedure outlined here but with a focus on improving the precision of calibration methods, refining the alignment techniques for stacking images, and conducting observations under more stable atmospheric conditions to minimize variability. Additionally, further studies could explore the complex history of globular cluster via spectroscopy to identify their chemical composition.

5 CONCLUSIONS

In this study, we have conducted a comprehensive analysis of the globular cluster M2, utilizing observations in the Johnsons Cousin's B and R filters. Our methodology involved precise data acquisition under optimal conditions and the implementation of a robust data reduction pipeline, which ensured the accuracy and reliability of our findings.

Our observations have led to the construction of a detailed Hertzsprung-Russell (HR) diagram, highlighting the effective temperatures and luminosities of the stars within M2. Through this, we identified multiple sub-branches within the Red Giant Branch (RGB), offering insights into the complex formation and evolutionary histories of the cluster.

However, our analysis also revealed potential sources of error, including calibration inaccuracies, frame misalignment, and atmospheric variability. These factors underscore the importance of continuous refinement in observational techniques and data reduction processes to enhance the precision of astronomical research.

The study of M2 has provided valuable insights into the properties and behaviours of globular clusters, contributing to our broader understanding of stellar evolution and galactic dynamics. Future research will aim to refine our methods further and explore additional clusters, such as M13, to build upon the findings presented here.

In summary, our research on M2 underscores the significance of detailed observational studies in advancing our knowledge of globular clusters. The comprehensive dataset and analysis techniques developed in this study lay a strong foundation for future investigations, promising further discoveries in the field of astronomy.

ACKNOWLEDGEMENTS

Thank you for the Grant that gave us the brand-new telescope in Glenlea. Thank you to the Judy and Jay Anderson for donating the ECO telescope to on UManitoba campus grounds. Thanks to Jade Yeung for creating the initial draft of the data reduction pipeline and lastly, thanks to Ryan Wierckx for venturing out to the site to gather the data.

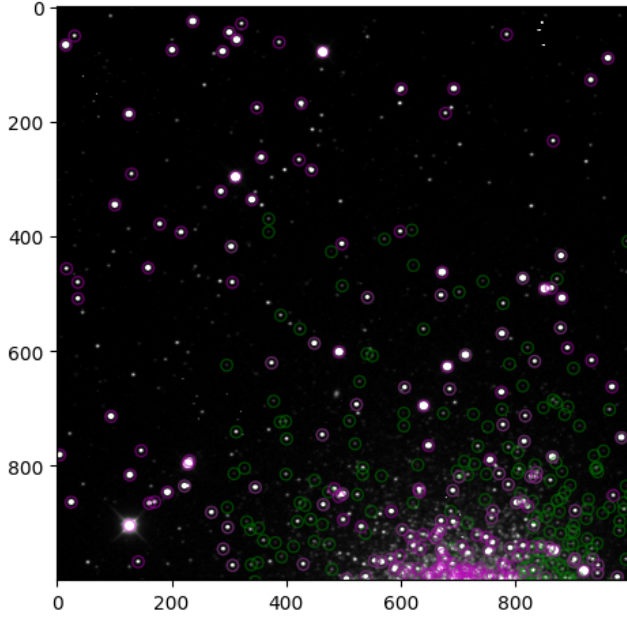


Figure A1. : Stetson's Catalog stars in green and detected peaked (DAOSTarFinder) in purple.

DATA AVAILABILITY

The images taken by Ryan was obtained from the UMLearn portal and should be available to students taking ASTR 3070 in the Fall of 2024. The Stetson's catalogue data was harvested from the Canadian Advanced Network for Astronomical Research (CANFAR). The pipeline code created by us is available at [Ahamed \(2024\)](#)

This paper has been typeset from a \LaTeX file prepared by the author.

REFERENCES

- Ahamed R. U., 2024, Observing M13, <https://github.com/TheRealCass/Observing-M13>
- Ballesteros F. J., 2012, EPL Volume 97, Number 3, February (2012)
- Gaudet et al., 2020, Stetson, Gaudet, séverin, <https://nrc-publications.canada.ca/eng/view/object/?id=9b885755-1783-4ae6-85e4-aad9e8eeddd6>
- Gratton R., Bragaglia A., Carretta E., D'Orazi V., Lucatello S., Sollima A., 2019, The Astronomy and astrophysics review, 27, 1
- Kuzma P. B., Da Costa G. S., Mackey A. D., Roderick T. A., 2016, Monthly notices of the Royal Astronomical Society, 461, 3639
- Lardo C., et al., 2013, Monthly notices of the Royal Astronomical Society, 433, 1941
- STETSON P. B., 1987, Publications of the Astronomical Society of the Pacific, 99, 191

APPENDIX A: SUPPORTING FIGURES

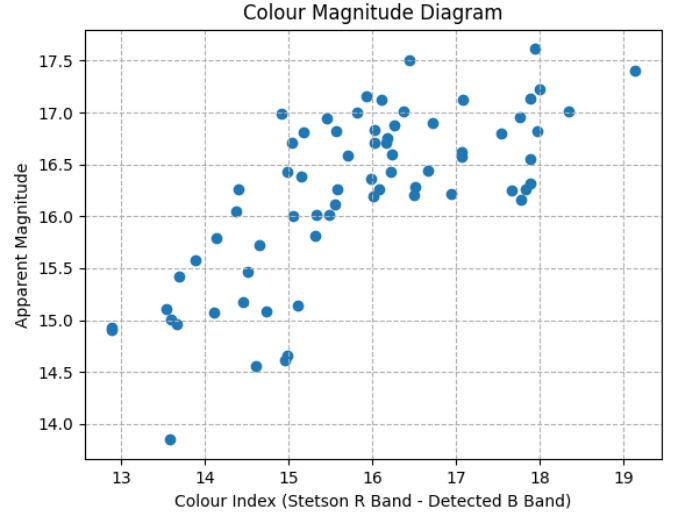


Figure A2. CMD from detected B band magnitude.

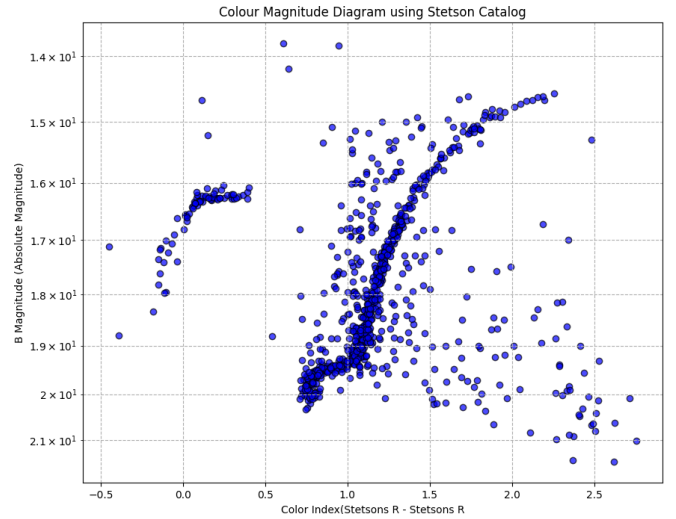


Figure A3. CMD from Stetson's B and R band magnitude.

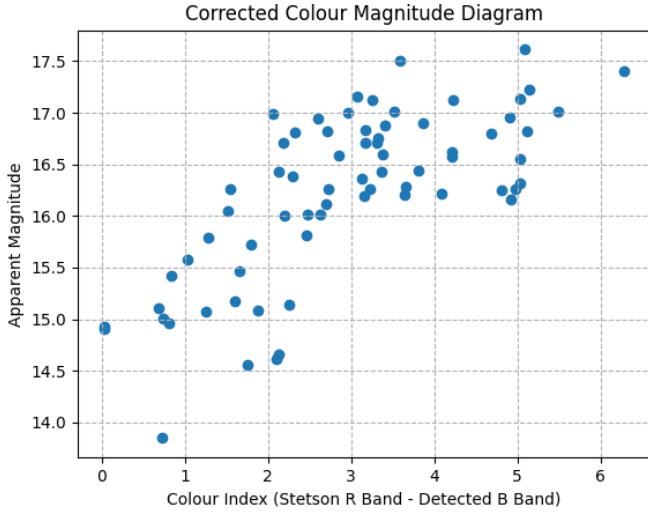


Figure A4. Corrected CMD.

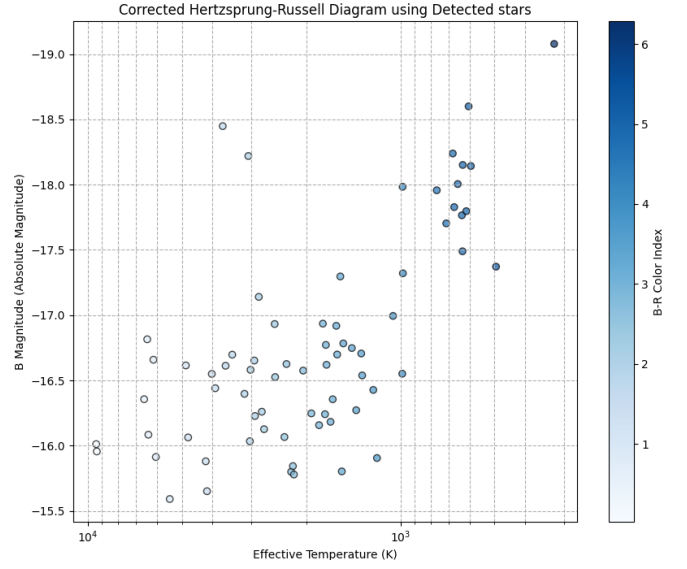


Figure A6. HR Diagram from detected magnitude with correction.

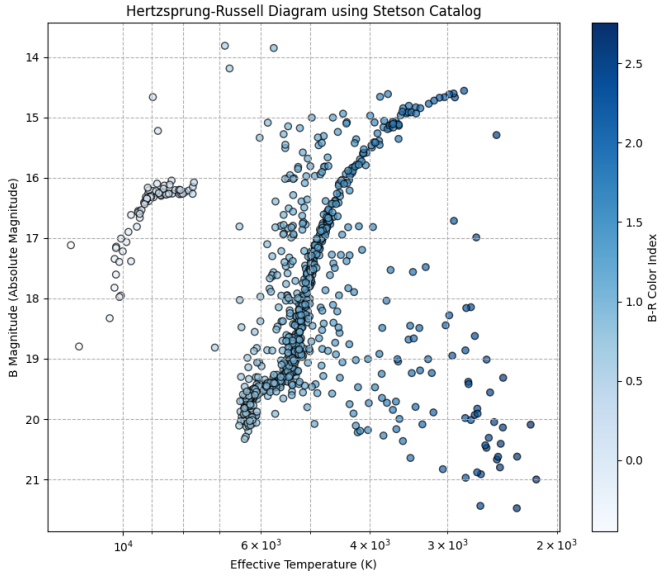


Figure A5. HR Diagram from Stetsons B and R band magnitude.

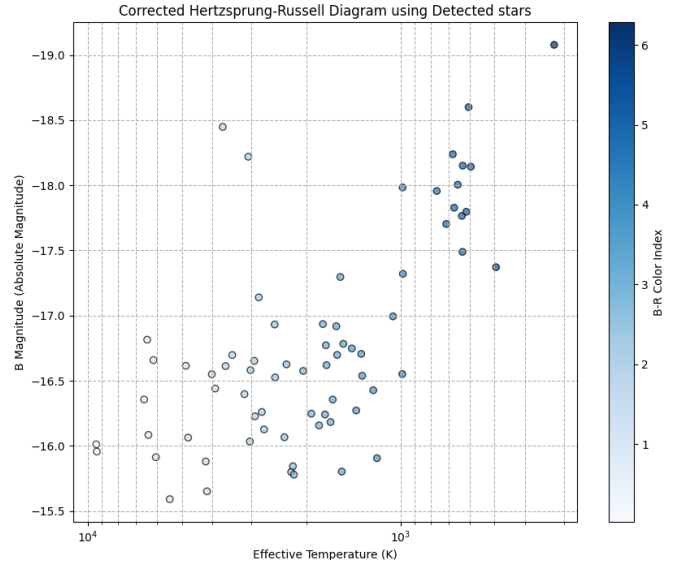


Figure A7. HR Diagram from detected B band magnitude.

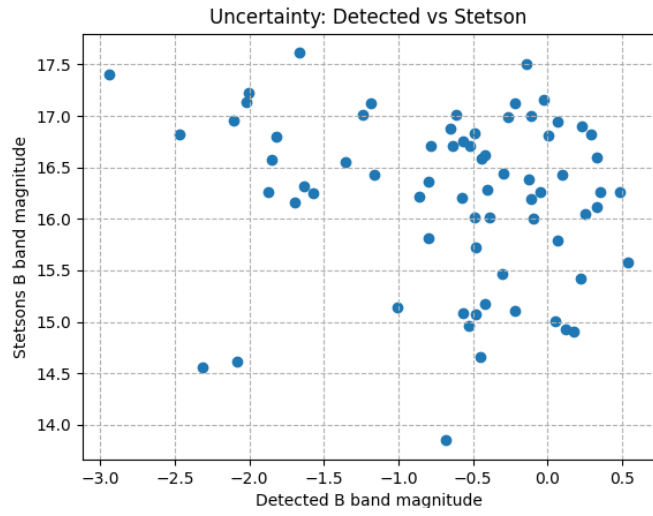


Figure A8. Uncertainty in detected vs stetson stars.

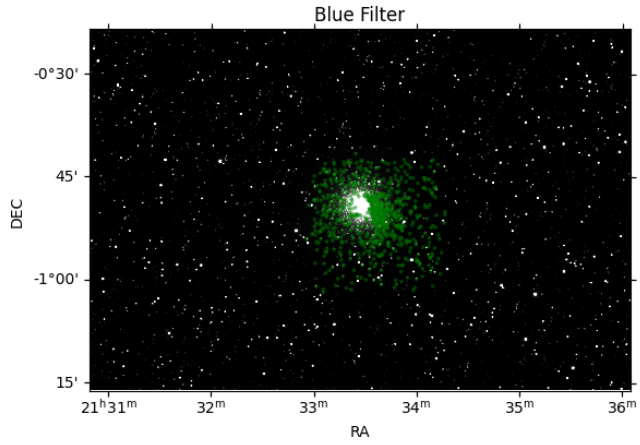


Figure A9. Stetson Catalogue stars overlayed on our FITS file.